



Study of the Effects Created by the Sunlight Passing Through the Rose Windows of Mallorca Cathedral

Albert Samper¹ · David Moreno-García¹ · Blas Herrera²

Accepted: 1 December 2023
© The Author(s) 2024

Abstract

This paper shows the light effects and geometric alignments created by the sunlight passing through the stained glasses of the eastern rose window in Mallorca Cathedral and projecting on the inner side of the cathedral's main façade and on the cathedral's floor. As well as providing more accurate information about these already known light effects, this paper makes use of laser scanning techniques and astronomical and geographical concepts in order to graphically display other novel effects which occur in coincidence with certain religious festivities throughout the year.

Keywords Mallorca Cathedral · Projection · Geometry · Light effect

Introduction

Throughout history, many buildings have been designed to interact with several celestial objects. Archaeoastronomy is the branch of science which studies these interactions, particularly in constructions dedicated to religious worship. Several examples can be cited which show how the design of certain constructions integrates the movement of stars: For instance, Magli (2016) reveals that the megalithic enclosure of Gobekli Tepe, probably the most ancient in the world, was designed to visualize the orbit of Sirius through the structures' orientation. Also, Catamo and Lucarini (2002) and Sigismondi (2012) describe the gnomon built by Francesco Bianchini in the Basilica of St. Mary of the Angels and of the Martyrs, which makes it possible to observe the meridian passage of the Sun and also of the stars Polaris, Arcturus and Sirius.

The star which has played the most relevant role in the history or architecture is the sun (Heilbron 1999; Torres 2000; Linares 2015). Due to its presence,

✉ Albert Samper
albert.samper@urv.cat

¹ Escola Tècnica Superior d'Arquitectura, Universitat Rovira i Virgili, Reus, Spain

² Departament de Enginyeria Informàtica y Matemàtiques, Universitat Rovira i Virgili, Tarragona, Spain

both light and shade effects and solstice and equinox alignments have been incorporated into the design of buildings, as seen for example in some religious constructions in Petra (Belmonte, González-García and Polcaro 2013), the Older Parthenon in Athens (Hannah 2013), or several places of worship (Heilbron 1999; González-García and Belmonte 2015; Ali and Cunich 2001).

This paper describes the light effects created by the sunlight passing through the stained glass of a rose window in Mallorca Cathedral. While it is well established that master builders were knowledgeable in astronomy and applied this knowledge to their buildings (Incerti 2013), the purpose of this paper is not to claim or deny that the architects who designed Mallorca Cathedral did so with such light effects or alignments in their minds. Using graphical tools and theoretical concepts of astronomy, this paper tries to show and explain the sunlight effects and geometric alignments which occur in this cathedral and involve its two main rose windows.

Sunlight Effects in Mallorca Cathedral

It is well known, particularly in Mallorca, that every year on the same dates, and almost at the same time, the morning sunlight passes through the giant eastern rose window and projects on the inner side of the main façade right underneath the western rose window, thus forming the celebrated ‘Eight Effect’ or ‘Festival of Light’ (Ruiz and Pol 2010). This light effect occurs every 2nd of February (Candlemas Day) and every 11th of November (Saint Martin of Tours) (see Fig. 1). These dates are 40 days and 43 days off Christmas, respectively, and the positions of both projections differ slightly.



Fig. 1 Sunlight effect which occurs every 2nd February inside the cathedral. Images: courtesy of Mallorca Cathedral

Also, in the days prior to the winter solstice, the sunlight passing through the eastern rose projects almost exactly on the western rose window, thus creating another light effect which can be seen from outside the cathedral (Fig. 2).

Even though these sunlight effects are widely known and appreciated by the visitors to the cathedral, their astronomical and geometric explanation is not commonly known. Therefore, for the purposes of research, the entire Mallorca cathedral has been digitalized and specific techniques were used in order to show the following time and geometric features, both mathematically and graphically, and make them common knowledge:

- (a) Accurate calculation of the moments in time when the projection of the eastern rose window is positioned underneath the western rose window on 2nd February and 11th November each year.
- (b) Accurate determination of the day and the moment in time when the projection of the eastern rose window comes closest to the center of the western rose window.
- (c) Daily path of the eastern rose window center projection on the inner side of the cathedral's main façade during certain religious festivities. Specifically: Epiphany (6th January), Candlemas (2nd February), All Saints' Day (1st November), All Souls Day (2nd November), St. Martin's Day (11th November), Solemnity of the Immaculate Conception (8th December), Winter Solstice Day (21st December) and Christmas Day (25th December). We have also considered the following traditional festivities in the island of Mallorca: St. Anthony (17th January) and St. Sebastian (20th January).
- (d) As a novelty, particular position of the eastern rose window's projection on the inner side of the cathedral's main façade on St. Luke's feast day (18th October) and St. Alexander's feast day (26th February).

Thus, in addition to providing more accurate information on light effects which are already widely known, this paper presents some novel effects created by the sunlight inside the Mallorca Cathedral (we consider these effects to be novel because they have been largely overlooked), as well as a graphical analysis of the eastern



Fig. 2 Sunlight effect which occurs in the days prior to the winter solstice, and can be seen from outside the cathedral. Images: courtesy of Mallorca Cathedral

rose window projection during certain religious festivities throughout the year. All our results are graphically displayed (floor plan and elevation) on the basis of strict astronomical criteria, as described in the following section.

Methods

Digital Reconstruction of Mallorca Cathedral

In order to calculate and graphically represent our results, it was necessary to create a digital model of the cathedral. Using a RTC360 Leica scanner, we carried out a laser scanner survey with 1250 stations and determined a cloud made up by 21,000,000 points covering the cathedral close and the space under consideration (Fig. 3).

In order to have a better graphic control of results and incorporate the numerical calculations into the architectural drawings, some parts of the building were outlined with CAD on the basis of the abovementioned survey (Figs. 4 and 5).

After this graphical analysis, the following parameters were established:

- Distance between the eastern rose window \mathcal{R}_E and the inner side of the cathedral's western façade σ : $\mathcal{L} = 75.954$ m.
- Height to the center \mathcal{C}_E of the eastern rose window \mathcal{R}_E and height to the center \mathcal{C}_P of the western rose window \mathcal{R}_P with respect to the central nave's floor level: $\mathcal{H}_E = 35.313$ m and $\mathcal{H}_P = 34.715$ m.
- Distance between \mathcal{O}_E , which is the orthogonal projection of \mathcal{C}_E on the wall σ , and the vertical axis containing \mathcal{C}_P : $\mathcal{D} = 0.141$ m.

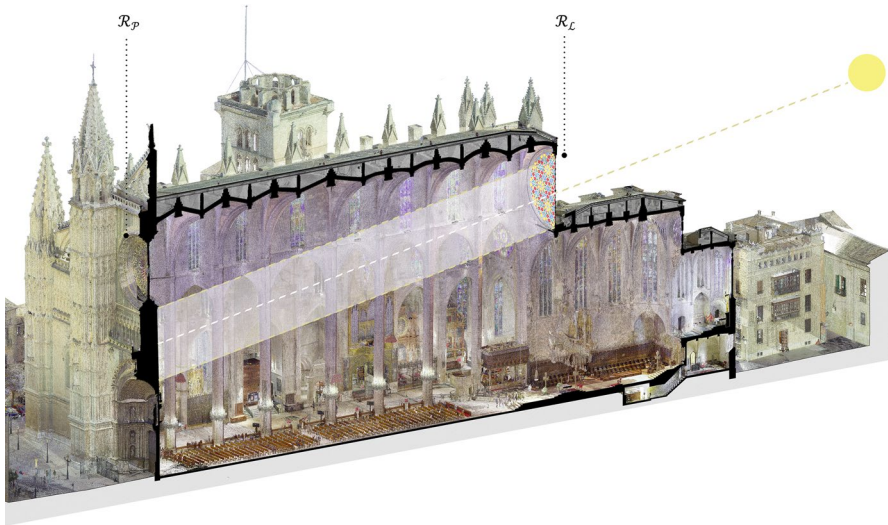


Fig. 3 Image of the resulting point cloud

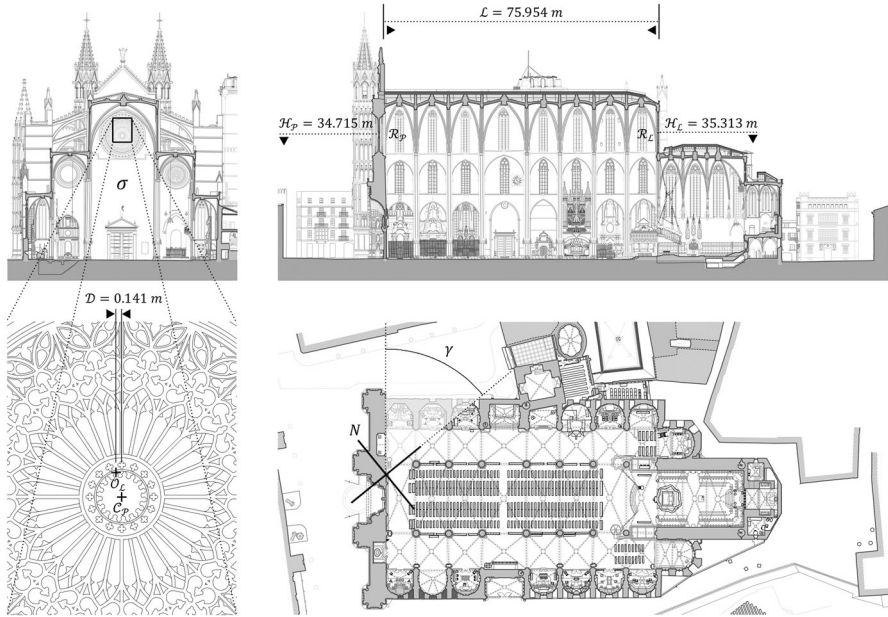


Fig. 4 Parameters considered in the paper

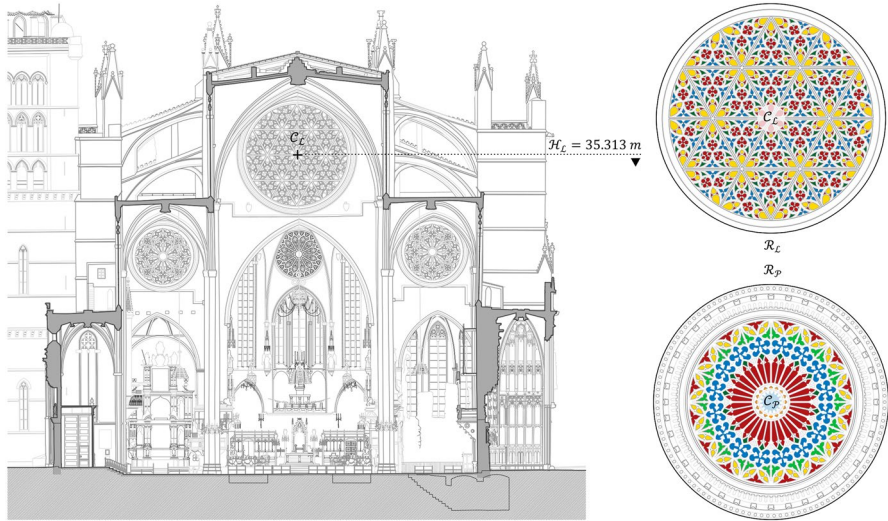


Fig. 5 Position of C_L on the eastern façade. Drawings of the rose windows which create the sunlight effects

- Amplitude of the angle formed between the inner side of the western façade and the equatorial plane in the direction of rotation north-east: $\gamma = 57.163^\circ$ sexagesimal degrees.

These parameters, together with the geographical location of the cathedral (latitude: $39^\circ 34' 02''.2N$, longitude: $2^\circ 38' 54''.9E$), are used to make the geometric calculations.

Astronomical and Geometric Explanation

The graphical results of this paper, presented in section "Results", are based on solving some astronomical and geometric problems. Assuming that the center θ_E of the earth is the center of the universe and also the center of a celestial sphere where the stars are, we need to: 1) determine the position θ_S of the center of the sun in the celestial sphere (apparent right ascension α_{app} and apparent declination δ_{app}) at every given instant JD , 2) determine the time equation E^m at the instant JD , and 3) determine the intersection $p_{\mathcal{L}} = \sigma \cap r_S$ of plane σ with the straight line r_S passing through $\mathcal{C}_{\mathcal{L}}$ and having the direction of vector $\overrightarrow{\theta_E \theta_S}$. Readers may turn to Martín (1990) and Meeus (1991) to learn in detail the definitions of the celestial positions, the time equation and all the concepts mentioned in this section.

In order to solve these problems, we use the well-known algorithms mentioned in Martín (1990) and Meeus (1991). The initial variable in these three problems is a calendar date.

Thus, we start from an initial variable date: year a , month $m \in \mathbb{Z} \cap (1, 12)$, day of the month d , hour h , minute m , second s , in Greenwich Civil Time, i.e., $GMT + 12^h$. Please note that in Mallorca, due to the delays and advancements imposed by the Spanish Government, we must consider the Greenwich Civil Time plus 1 hour in Autumn-Winter or plus 2 hours in Spring-Summer.

Next, the date is converted to Julian Date JD . Readers may turn to Martín (1990) and Meeus (1991) for definitions and calculations of: CE Gregorian year (from 14th October 1582 onwards), CE and BCE Julian year (until 4th October 1582), and Julian Day JD (#) according to the time measurement system proposed by Joseph Scaliger.

Meeus (1991) provides the following algorithm to calculate JD when $JD > 0$: Let $D = d + \frac{h}{24} + \frac{m}{1440} + \frac{s}{86400}$. If $m > 2$, a and m remain unchanged. If $m \leq 2$, a is replaced by $a - 1$ and m is replaced by $m + 12$. Thus, if $JD > 0$, in CE Gregorian year we have that $JD = [365.25(a + 4716)] + [30.6001(m + 1)] + 2 - \left\lfloor \left(\frac{a}{100} \right) \right\rfloor + \left\lfloor \frac{\left\lfloor \frac{a}{100} \right\rfloor}{4} \right\rfloor + D - 1524.5$, and in CE Julian year we have that $JD = [365.25(a + 4716)] + [30.6001(m + 1)] + D - 1524.5$, where $[x] = \max\{k \in \mathbb{Z} \text{ with } k \leq x\}$.

Calculating the Position of the Sun in the Celestial Sphere

Now that we know JD , we can calculate δ_{app} , which is the apparent declination of the Sun in the celestial sphere. We will use the algorithms in Meeus (1991) with an error of $0.01''$ sexagesimal seconds. Even though we do not need such level of accuracy for our purposes, we follow the steps and calculate the following astronomical variables:

- (a) T , the time in Julian centuries of 36525 ephemeris days, measured from the Julian epoch $J2000.00$, which corresponds to the date 2000 January 1.5 in Dynamical Time DT : $T = \frac{JD-2451545.00}{36525}$.
- (b) L_0 , geometric mean longitude of the Sun referred to the mean equinox of date T : $L_0 = 280^\circ.46646 + 36000^\circ.76983T + 0^\circ.0003032T^2$.
- (c) M , the mean anomaly of the Sun: $M = 357^\circ.52911 + M = 357^\circ.52911 + 35999^\circ.05029T - 0^\circ.0001537T^2$.
- (d) e , the eccentricity of the Earth's orbit: $e = 0.016708634 - 0.000042037T - 0.0000001267T^2$.
- (e) C , the equation of the Center of the Sun: $C = (1^\circ.914602 - 0^\circ.004817T - 0^\circ.000014T^2) \sin M + (0^\circ.019993 - 0^\circ.000101T) \sin (2M) + 0^\circ.000289 \sin (3M)$.
- (f) \odot , the true geometric longitude of the Sun referred to the mean equinox of date T : $\odot = L_0 + C$.
- (g) $\Omega = 125^\circ.04452 - 1934^\circ.136621T$.
- (h) λ , the apparent longitude of the Sun referred to the true equinox of date T , correcting for nutation and aberration: $\lambda = \odot - 0^\circ.00569 - 0^\circ.00478 \sin \Omega$.
- (i) ϵ_0 , the mean obliquity of the ecliptic: $\epsilon_0 = 23^\circ 26' 21''.448 - 46''.8150T - 0''.00059T^2 + 0''.001813T^3$.
- (j) L' , the mean longitude of the Moon: $L' = 218^\circ.3165 + 481267^\circ.8813T$.
- (k) $\Delta\epsilon$, the nutation in obliquity of the ecliptic: $\Delta\epsilon = 9''.20 \cos \Omega + 0''.57 \cos (2L_0) + 0''.10 \cos (2L') - 0''.09 \cos (2\Omega)$.
- (l) ϵ , the true obliquity of the ecliptic: $\epsilon = \epsilon_0 + \Delta\epsilon$.
- (m) δ_{app} , the apparent declination of the Sun: $\delta_{app} = \sin^{-1} (\sin \epsilon \sin \lambda)$, calculated in sexagesimal degrees.

Calculating the Time Equation

Next, given the date JD , we proceed to calculate the time equation E^m . Again, we use the algorithms provided in Meeus (1991) to calculate the following astronomical variables:

- (a) The sum of the mean value of the aberration in longitude and the correction for reduction to the FK5 system: $0^\circ.0057183 = -20''.49552 - 0''.09033$.

- (b) $\Delta\psi$, the nutation in longitude of the ecliptic: $\Delta\psi = -17''.20 \sin \Omega - 1''.32 \sin (2L_0) - 0''.23 \sin (2L') + 0''.21 \sin (2\Omega)$.
- (c) α_{app} , the apparent right ascension of the Sun taking into account the aberration and the nutation: $\alpha_{app} = \tan^{-1} \left(\frac{\cos \varepsilon \sin \lambda}{\cos \lambda} \right)_2$, calculated in sexagesimal degrees.
- (d) If $\alpha_{app} < 0$, then: $A_{app} = \left(\frac{\alpha_{app}}{360} - \left\lfloor \frac{\alpha_{app}}{360} \right\rfloor - 1 \right) * 360 + 360$.
- (e) If $\alpha_{app} \geq 0$, then: $A_{app} = A_{app} = \left(\frac{\alpha_{app}}{360} - \left\lfloor \frac{\alpha_{app}}{360} \right\rfloor \right) * 360$.
- (f) If $L_0 < 0$, then: $l_0 = \left(\frac{L_0}{360} - \left\lfloor \frac{L_0}{360} \right\rfloor - 1 \right) * 360 + 360$.
- (g) If $\alpha_{app} \geq 0$, then: $l_0 = \left(\frac{L_0}{360} - \left\lfloor \frac{L_0}{360} \right\rfloor \right) * 360$.
- (h) E , the time equation: $E = l_0 - 0^\circ.0057183 - A_{app} + \Delta\psi \cos \varepsilon$, calculated in sexagesimal degrees.
- (i) E^m , the time equation: $E^m = 4E$, calculated in minutes of time. We know that $|E^m| < 20^m$, i.e., the equation of time is always less than 20 minutes in absolute value. Therefore, if the calculation of $|E^m|$ renders a value larger than 20, then we will add or subtract a convenient multiple of 24^h .

Since α_{app} is in the same quadrant as λ , the function $\tan^{-1} \left(\frac{A}{B} \right)_2$ is defined in a particular manner which the reader may find in Meeus (1991).

Calculating the Geometric Projection

Having calculated δ_{app} and E^m based on JD , the required parameters are gathered from subsection "[Digital reconstruction of Mallorca Cathedral](#)" in order to carry out the solar projection of $\mathcal{C}_{\mathcal{L}}$ on the plane σ and determine the point $p_{\mathcal{L}}$. Cartesian orthonormal reference system $\{\theta; \vec{e}_1, \vec{e}_2, \vec{e}_3\}$ is used, such that a) if points in space have coordinates (x, y, z) , then the equation of plane σ is $x=0$, b) \vec{e}_3 has direction towards the zenith, c) \vec{e}_1 has direction towards $\mathcal{C}_{\mathcal{L}}$, d) \vec{e}_2 is such that the base $\vec{e}_1, \vec{e}_2, \vec{e}_3$ is clockwise (i.e., if \vec{e}_1 pointed south, \vec{e}_2 would point west), and e) $(0,0,0)$ are the coordinates of $\mathcal{O}_{\mathcal{L}}$, which is the orthogonal projection of $\mathcal{C}_{\mathcal{L}}$ on σ . Using the algorithms described in Martín (1990) and Meeus (1991), the following geometric parameters are calculated in order to determine $p_{\mathcal{L}}$.

- (a) h_s , solar time. Taking into account the time equation E^m and the geographical longitude of the cathedral $lon = 2^\circ 38' 54''.9E = -2^\circ.785833$, we determine the solar time in Mallorca: $h_s = h + \frac{m}{60} + \frac{s}{360} - \frac{24}{360} * lon + \frac{E^m}{60}$.
- (b) $\beta = 90 - lat$, where the geographical latitude of the cathedral is $lat = 39^\circ 34' 02''.2N = 39^\circ.572777$.
- (c) $H = 360 \frac{h_s - 12}{24}$.
- (d) $Azimuth = \tan^{-1} \left(\frac{\sin H}{\cos(H) \cos \beta - \tan(\delta_{app}) \sin \beta} \right)$.
- (e) $Height = \sin^{-1} (\sin \beta \cos(\delta_{app}) \cos H + \cos \beta \sin(\delta_{app}))$.
- (f) $\mu = \frac{-x_0}{(\cos(Azimuth) \cos \gamma + \sin(Azimuth) \sin \gamma) \cos(Height)}$, where $x_0 = 75.954$.

- (g) $y_1 = \mu(-\cos(\text{Height})\cos(\text{Azimuth})\sin\gamma + \cos(\text{Height})\sin(\text{Azimuth})\cos\gamma)$.
 (h) $z_1 = \mu\sin(\text{Height})$.

After the above steps, the coordinates of the projection of $C_{\mathcal{L}}$ are determined. Such coordinates are: $p_{\mathcal{L}} = (0, y_1, z_1)$. The variation of this projection $p_{\mathcal{L}}$ over time results in paths $\mathcal{T}_{i/j}$ on the plane σ . These paths are graphically described below.

Similarly, the intersection $q_{\mathcal{L}} = \rho \cap r_S$ is determined. This is the intersection of plane ρ , which is the floor plane, and the straight line r_S passing through $C_{\mathcal{L}}$ and having the direction of vector $\overline{\theta_E\theta_S}$. In order to do that, the last three steps above f), g), h) are modified as follows:

- (1) $\mu = \frac{-35.313}{\sin(\text{Height})}$.
 (2) $x_1 = x_0 + \mu(\cos(\text{Height})\cos(\text{Azimuth})\cos\gamma + \cos(\text{Height})\sin(\text{Azimuth})\sin\gamma)$.
 (3) $y_1 = \mu(-\cos(\text{Height})\cos(\text{Azimuth})\sin\gamma + \cos(\text{Height})\sin(\text{Azimuth})\cos\gamma)$.

After the above steps, the coordinates of the projection $q_{\mathcal{L}}$ of $C_{\mathcal{L}}$ on the floor plane ρ are determined. Such coordinates are: $q_{\mathcal{L}} = (x_1, y_1, -35.313)$. The variation of this projection $q_{\mathcal{L}}$ over time results in paths $\mathcal{L}_{i/j}$ on the plane ρ . These paths are graphically described below.

Results

Using the abovementioned astronomical and geometric algorithms (which were programmed in C++ by the authors for better numeric accuracy), the points $p_{\mathcal{L}}$ are obtained which describe the daily paths $\mathcal{T}_{i/j}$ generated by the projection of $C_{\mathcal{L}}$ on the plane σ ; and the points $q_{\mathcal{L}}$ are obtained which describe the daily paths $\mathcal{L}_{i/j}$ generated by the projection of $C_{\mathcal{L}}$ on the cathedral's floor plane ρ . These daily paths $\mathcal{T}_{i/j}$, corresponding to the dates listed in Table 1, are graphically represented in Figs. 6, 7 and 8; and the daily paths $\mathcal{L}_{i/j}$ are graphically represented in Fig. 9.

Besides, in order to provide the reader with more information, the previous Fig. 6, 7 and 8 show (in orange and left to right) the analemmas for 7.00 am, 8.00 am and 9.00 am in Greenwich Civil Time. Figure 9 below shows (in orange) the analemmas for 8.00 am, 9.00 am and 10.00 am in Greenwich Civil Time.

Conclusion

The following considerations can be made about the light effects which are graphically displayed in section "Results".

Considerations about the commonly known sunlight effects:

- (a) On the 11th of November (St. Martin of Tours) at 8.33 am $C_{\mathcal{L}}$ is projected on the vertical straight line passing through the center of $\mathcal{R}_{\mathcal{P}}$; the distance between $p_{\mathcal{L}}$

Table 1 Paths $\mathcal{T}_{i/j}$ and $\mathcal{L}_{i/j}$ calculated for the above dates of the year 2022, Julian Day at 12:00 h

Figures	$\mathcal{T}_{i/j}$	Festivity	Day in the Gregorian calendar	Julian Day $JD(\#)$
6	$\mathcal{T}_{2/2}$	Candlemas	2nd February	2459613
6	$\mathcal{T}_{11/11}$	St. Martin of Tours	11th November	2459895
7	$\mathcal{T}_{6/1}$	Epiphany	6th January	2459586
7	$\mathcal{T}_{1/11}$	All Saints' Day	1st November	2459885
7	$\mathcal{T}_{2/11}$	All Souls Day	2nd November	2459886
7	$\mathcal{T}_{8/12}$	Immaculate Conception	8th December	2459922
8	$\mathcal{T}_{21/12}$	Winter Solstice	21st December	2459935
8	$\mathcal{T}_{25/12}$	Christmas	25th December	2459939
8	$\mathcal{T}_{17/1}$	St. Anthony	16th January	2459596
8	$\mathcal{T}_{20/1}$	St. Sebastian	19th January	2459599
8	$\mathcal{T}_{18/10}$	St. Luke	18th October	2459871
8	$\mathcal{T}_{26/2}$	St. Alexander	26th February	2459637
9	$\mathcal{L}_{19/3}$	St. Joseph	19th March	2459658
9	\mathcal{L}_e	Spring Equinox	20th March	2459659
9	\mathcal{L}_e	Autumn Equinox	23rd September	2459846
9	$\mathcal{L}_{25/3}$	Annunciation of the Lord	25th March	2459664
9	$\mathcal{L}_{8/9}$	Nativity of the Virgin Mary	8th September	2459831
9	$\mathcal{L}_{15/8}$	Assumption of the Virgin Mary	15th August	2459807
9	$\mathcal{L}_{31/5}$	Visitation of the Virgin Mary	31st May	2459731
9	$\mathcal{L}_{21/6}$	Summer Solstice	21st June	2459752

and \mathcal{C}_p is 13.05 meters. Similarly, on the 2nd of February (Candlemas Day) at 9.03 am \mathcal{C}_L is projected on the vertical straight line passing through the center of \mathcal{R}_p ; the distance between p_L and \mathcal{C}_p is 14.19 m. Thus, the 'Eight Effect' is more clearly visible on St. Martin's Day (cf. Fig. 6).

- (b) On 2nd February at 9.03 am the projection of \mathcal{C}_L on the plane σ is exactly at half the distance between the cathedral's floor level and the height of the topmost point in the edge of the rose window \mathcal{R}_p (cf. Fig. 6). This middle point lies at a height of 20.61 meters.
- (c) The paths $\mathcal{T}_{21/12}$, $\mathcal{T}_{25/12}$, $\mathcal{T}_{8/12}$ and $\mathcal{T}_{6/1}$ cross the stained glasses of the western rose window between 8.00 am and 8.30 am. Due to this, the sun rays passing through \mathcal{R}_L are projected onto \mathcal{R}_p , illuminating it from the inside of the cathedral. This effect is strongest on Winter Solstice Day at 8:17 am, when the distance between \mathcal{C}_p and the path $\mathcal{T}_{21/12}$ is the shortest (1.31 meters) (cf. Figs. 7 and 8).

Considerations about other sunlight effects which are not commonly known:

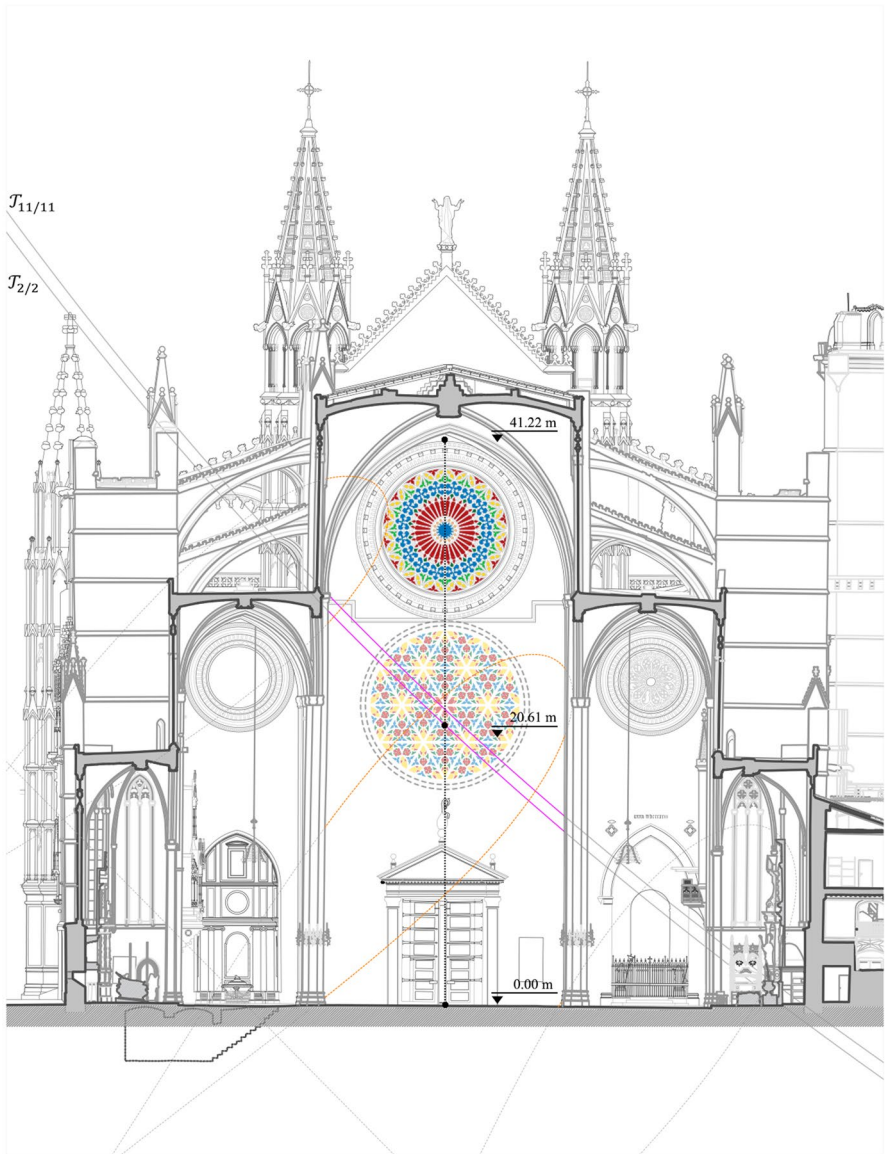


Fig. 6 Graphical representation of $T_{11/11}$ and $T_{2/2}$ on the plane σ

- (d) On the 1st and 2nd of November at 8.45 am C_L is projected onto the ornamental element located on top of the frieze which crowns the main entrance porch to the cathedral. The mean distance between both projections p_L and this element is 0.89 meters (cf. Fig. 8).
- (e) On 17th January and on 20th January at 9.03 am the projection of C_L on the plane σ is positioned exactly at two thirds of the distance between the cathedral's floor

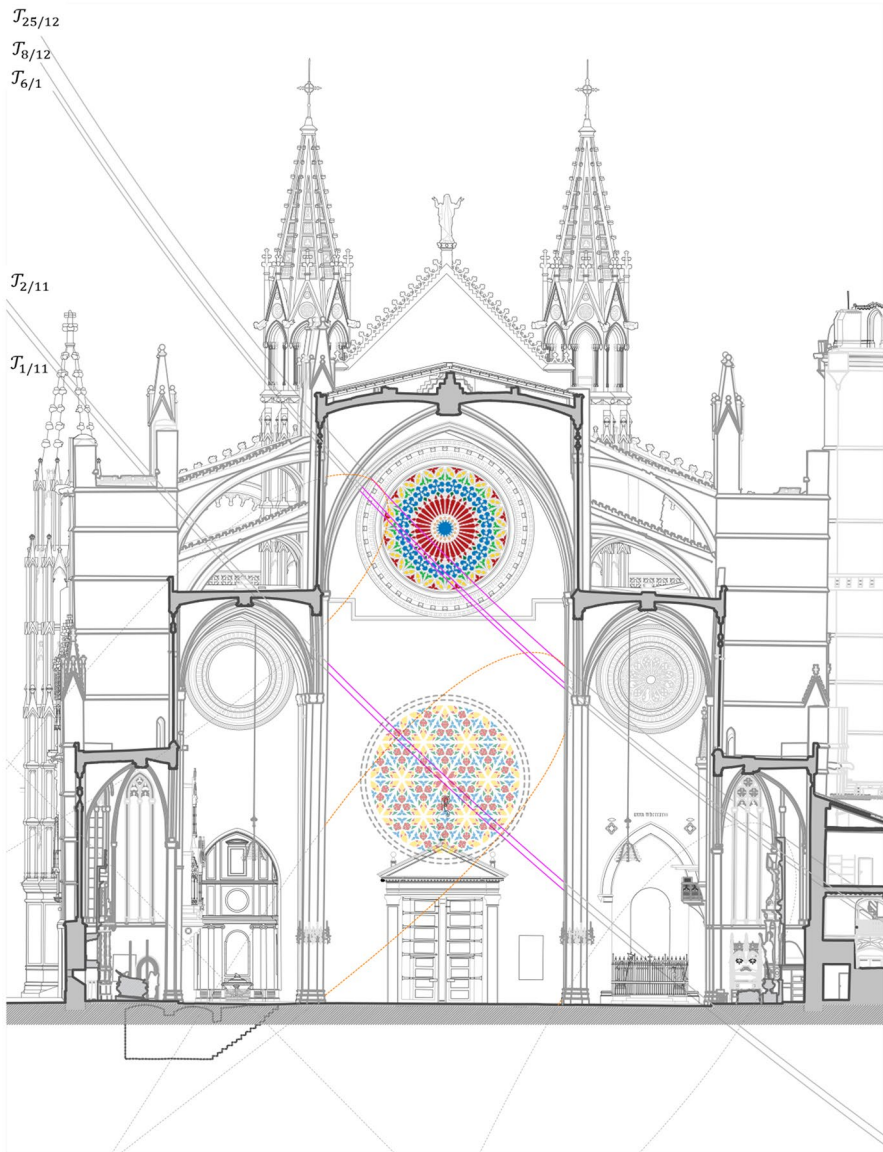


Fig. 7 Graphical representation of $J_{25/12}$, $J_{8/12}$, $J_{6/1}$, $J_{2/11}$ and $J_{1/11}$ on the plane σ

level and the height of the topmost point in the edge of the rose window \mathcal{R}_p (cf. Fig. 8). This position lies at a height of 27.48 meters.

- (f) As shown in figure 8, on the 18th of October at 10.03 am and on the 26th of February at 9.31 am the rose window \mathcal{R}_c is projected exactly onto the access door to the cathedral. On 18th October, this projection is even tangent to the horizontal plane of the cathedral.

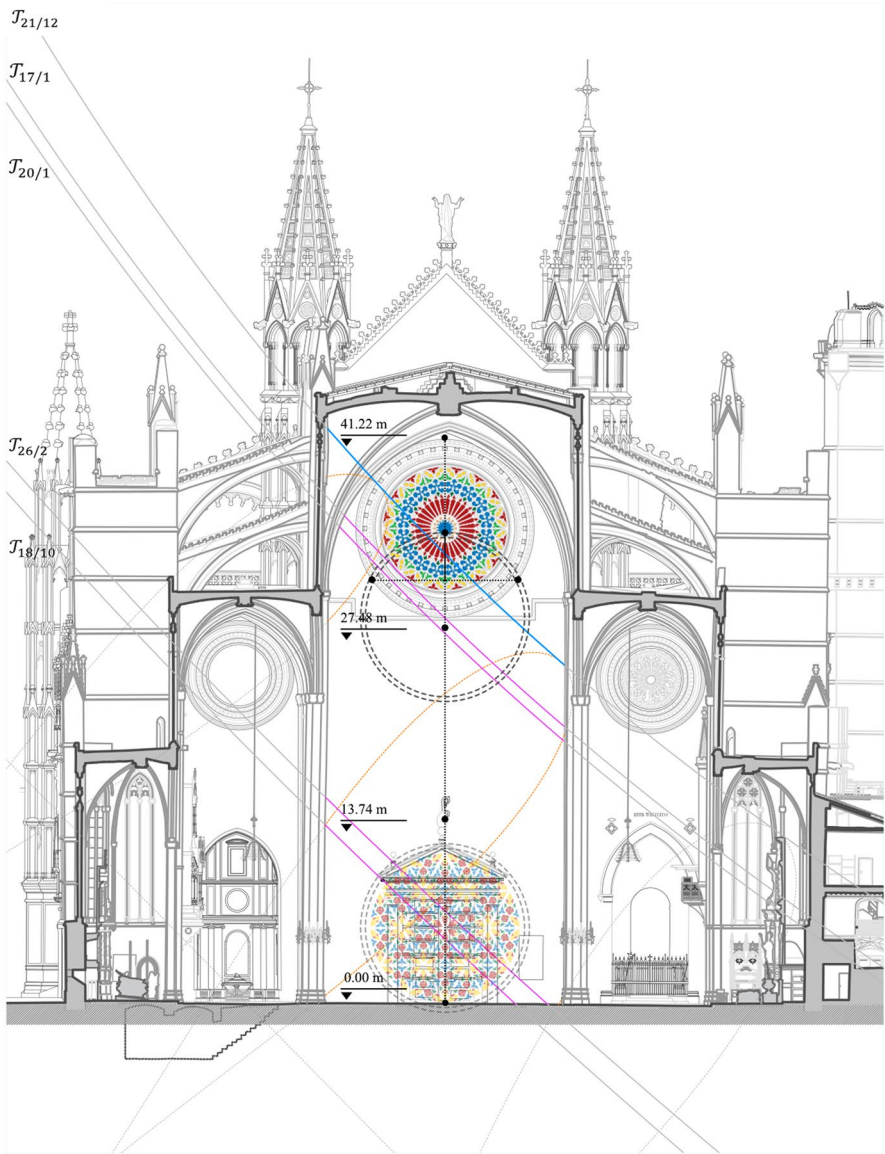


Fig. 8 Graphical representation of $T_{21/12}$, $T_{17/1}$, $T_{20/1}$, $T_{26/2}$ and $T_{18/10}$ on the plane σ

With regard to the projections of the eastern rose window \mathcal{R}_L on the cathedral's floor plane ρ , no significant relationship can be observed between the solar paths and the architectural elements. However, it should be noted that between March and June, the projection of this rose window illuminates a larger area of pavement than during the rest of the year.

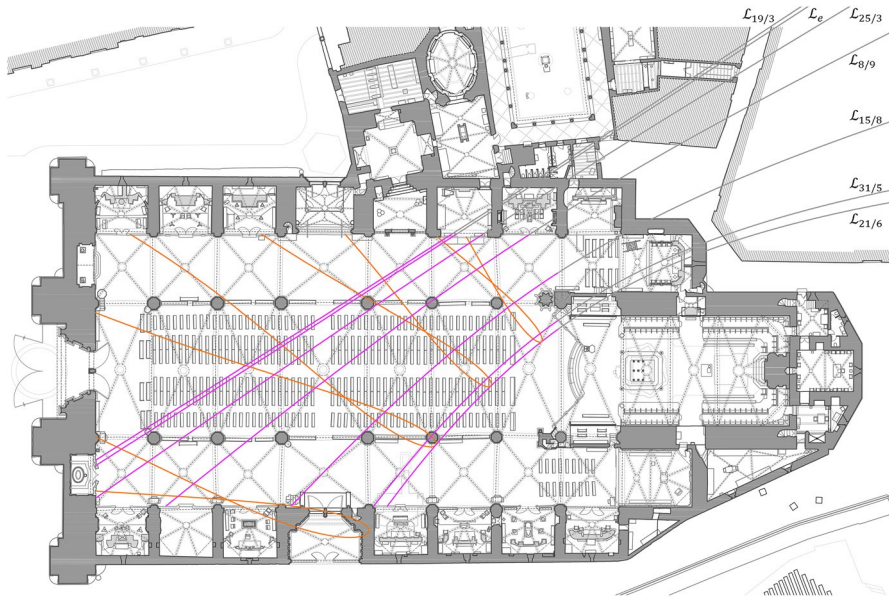


Fig. 9 Graphical representation of $\mathcal{L}_{19/3}$, \mathcal{L}_e , $\mathcal{L}_{25/3}$, $\mathcal{L}_{8/9}$, $\mathcal{L}_{15/8}$, $\mathcal{L}_{31/5}$ and $\mathcal{L}_{21/6}$ on the cathedral's floor plane ρ

In summary, this paper makes use of laser scanning techniques and astronomical and geometric concepts in order to graphically display the light effects and alignments (both known and unknown) which occur when the sunlight passes through the stained glasses of the eastern rose window in Mallorca Cathedral and projects this rose window on the inner side of the cathedral's main façade.

Funding Open Access funding provided thanks to the CRUE-CSIC agreement with Springer Nature.

Open Access This article is licensed under a Creative Commons Attribution 4.0 International License, which permits use, sharing, adaptation, distribution and reproduction in any medium or format, as long as you give appropriate credit to the original author(s) and the source, provide a link to the Creative Commons licence, and indicate if changes were made. The images or other third party material in this article are included in the article's Creative Commons licence, unless indicated otherwise in a credit line to the material. If material is not included in the article's Creative Commons licence and your intended use is not permitted by statutory regulation or exceeds the permitted use, you will need to obtain permission directly from the copyright holder. To view a copy of this licence, visit <http://creativecommons.org/licenses/by/4.0/>.

References

Ali, Jason, and Peter Cunich. 2001. The Orientation of Churches: Some New Evidence. *Antiquaries Journal* 81: 155-193. <https://doi.org/10.1017/S0003581500072188>

- Belmonte, Juan Antonio, César González-García and Andrea Polcaro. 2013. Light and Shadows over Petra: Astronomy and Landscape in Nabataean Lands. *Nexus Network Journal* 15: 487-501. <https://doi.org/https://doi.org/10.1007/s00004-013-0164-6>.
- Catamo, Mario and Cesare Lucarini. 2002. *Il cielo in Basilica. La Meridiana della Basilica di Santa Maria degli Angeli e dei Martiri in Roma*. Roma: Edizioni AGAMI.
- González-García, César and Juan Antonio Belmonte. 2015. The Orientation of Pre-Romanesque Churches in the Iberian Peninsula. *Nexus Network Journal* 17: 353-377. <https://doi.org/https://doi.org/10.1007/s00004-014-0231-7>.
- Hannah, R. 2013. Greek Temple Orientation: The Case of the Older Parthenon in Athens. *Nexus Network Journal* 15: 423-443. <https://doi.org/https://doi.org/10.1007/s00004-013-0169-1>.
- Heilbron, John Lewis. 1999. *The Sun in the Church: Cathedrals as Solar Observatories*. Harvard: Harvard University Press.
- Incerti, M. 2013. Astronomical Knowledge in the Sacred Architecture of the Middle Ages in Italy. *Nexus Network Journal* 15: 503-526. <https://doi.org/https://doi.org/10.1007/s00004-013-0167-3>.
- Linares, O. 2015. Precisiones sobre la luz en el Pantheon de Roma. *VLC arquitectura* 2(1): 33-55. <https://doi.org/https://doi.org/10.4995/vlc.2015.3376>.
- Magli, G. 2016. Sirius and the project of the megalithic enclosures at Gobekli Tepe. *Nexus Network Journal* 18: 337-346. <https://doi.org/https://doi.org/10.1007/s00004-015-0277-1>.
- Martín, F. 1990. *Astronomía*. Madrid: Parainfo.
- Meeus, J. 1991. *Astronomical Algorithms*. Richmond: Willmann-Bell, Inc.
- Ruiz, Daniel and Josep-Lluís Pol. 2010. Els efectes de la llum solar a la seu de Mallorca. *Actes d'història de la ciència i de la tècnica, Nova Època*, 3(1): 37-47.
- Sigismondi, C. 2012. Measuring the position of the center of the Sun at the Clementine Gnomon of Santa Maria degli Angeli in Rome. *Journal for Occultation Astronomy* 1: 20-23. <https://doi.org/https://doi.org/10.48550/arXiv.1201.0510>.
- Torres, Elías. 2000. *Luz cenital*. Barcelona: Editorial Col·legi Oficial d'Arquitectes de Catalunya.

Publisher's Note Springer Nature remains neutral with regard to jurisdictional claims in published maps and institutional affiliations.

Albert Samper is an Architect who obtained his Ph.D. in Architecture at the University of Rovira i Virgili in 2014. Presently, he is an Assistant Professor of Architecture at the same university and his main fields of interest are architectural heritage, architectural representation and the application of geometry to architecture.

David Moreno-García is an architect and Ph D student at the University of Rovira I Virgili in 2014. Presently, he is an Associate Professor of Architecture at the same university and his main fields of interest are architectural heritage and architectural representation. He has collaborated in the realization of the three-dimensional modeling, with point cloud techniques, of the Cathedral of Mallorca, the Cathedral of Gerona and the Cathedral of Narvona.

Blas Herrera is Geometer who obtained his D.Sc. in Mathematics at the Autònoma University of Barcelona in 1994. Presently, he is a full Professor of Applied Mathematics at the University of Rovira i Virgili. His main fields of research interest are classical geometry, differential geometry and the application of geometry to architecture, fluid mechanics and engineering.